Introducing Dynamic Demand Response in the LFC Model

S. Ali Pourmousavi, *Student Member, IEEE*, M. Hashem Nehrir, *Life Fellow, IEEE*

***Abstract*— Demand response (DR) has proved to be an inevitable part of the future grid. Much research works have been reported in the literature on the benefits and implementation of DR. However, little works have been reported on the impacts of DR on dynamic performance of power systems, specifically on the load frequency control (LFC) problem. This paper makes an attempt to fill this gap by introducing a DR control loop in the traditional LFC model (called LFC-DR) for a single-area power system. The model has the feature of optimal operation through optimal power sharing between DR and supplementary control. The effect of DR communication delay in the controller design is also considered. It is shown that the addition of the DR control loop increases the stability margin of the system and DR effectively improves the system dynamic performance. Simulation studies are carried out for single-area power systems to verify the effectiveness of the proposed method.**

***Index Terms*—Demand response (DR), linear quadratic regulator (LQR), single-area power system model, sensitivity, smart grid, stability, steady-state error.**

I. Introduction

TRADITIONALLY, frequency regulation in power system is achieved by balancing generation and demand through load following, i.e., spinning and non-spinning reserves [1]. The future power grid, on the other hand, is foreseen to have high penetration of renewable energy (RE) power generation, which can be highly variable. In such cases, energy storage and responsive loads show great promise for balancing generation and demand, as they will help to avoid the use of the traditional generation following schemes, which can be costly and/or environmentally unfriendly.

Given the limited availability, low efficiency, and high cost of large storage devices, real-time smart responsive load participation, known as demand response (DR), has been actively considered for power balancing. It can be achieved by active consumer participation in real-time to maintain balance between generation and demand with two-way communication [2]. It is well known that DR increases system reliability and flexibility to manage the variability and uncertainty of some RE resources, decreases the cost of operation, and enhances system efficiency. Furthermore, DR can be used to provide ancillary services (AS) for regulation reserve and to respond momentarily to the area control error (ACE). Although AS are called more frequently than traditional load shedding events, the annual total hours of curtailment is much less, and individual events are much shorter. Thus, AS programs may appeal to retail customers, as they will find more frequent and short on/off switching of some of their end-use loads more acceptable than infrequent and long curtailments [3]. Examples of customer end-use loads that have instantaneous response and are potential candidates for DR are electric water heaters (EWHs) and HVACs. For the above reasons considerable attention has been recently given to DR for different purposes, e.g. economic benefits of DR [4]-[8], off-line planning and day-ahead scheduling [9]-[15], availability assessment of the DR resources for reserve capacity [16]-[18], and analysis of the effectiveness of DR in providing AS at the islanded distribution-level microgrids [19]-[21]. A number of studies have also addressed the effectiveness of decentralized dynamic demand control on stabilization of grid frequency, mainly at the transmission level [22]-[31]. However, the above studies present the following shortcomings:

- They do not present a general framework for the analysis of the impacts of DR on a general power system model and load [22]-[28], [30], and [31]
- AGC model has not been considered in the analysis, [22], [24]-[28], and [30]
- Only specific loads (such as HVAC, EWHs and lighting) have been considered in [23], [24], [27] and specific power systems without generalization, [22], [23], [25]-[28], and [30]
- Communication delay in central DR, and measurement delay in decentralized DR have not been considered, [22]-[26], [30], and [31]
- Frequency regulation as AS have not been studied. Only under-frequency load shedding (UFLS) characterization has been analyzed, [30], [31]
- Unreal assumptions for the availability of DR at all times have been made, [29]
- Load-damping coefficient, which can improve frequency stabilization, has been ignored, [27]
- Only sensitivity analysis of frequency-related load-damping coefficient characteristic without generalization and DR control is presented, [31]

In the last five decades, traditional LFC models have been revised and modified to include the different types of power

This work was supported by the DOE Award DE-FG02-11ER46817, and by Montana State University.

S.A. Pourmousavi (email: s.pourmousavikani@msu.montana.edu), and M.H. Nehrir (email: hnehrir@ece.montana.edu) are with the Electrical and Computer Engineering Department, Montana State University, Bozeman, 59717 USA.

plants, including RE power generation with actual limitations, such as ramp-up/down limits, in the traditional and de-regulated power market [32]-[33]. These models are useful in small disturbance studies such as small variations in load and generation, and in controller design. However, so far in the literature, the concept of control in the LFC model has only focused on the generation side, and DR has not been included in these studies. In this paper we modify the general small-signal model of a power system used in LFC studies by introducing a DR control loop to the LFC model (called LFC-DR).

Other goals of the paper are to make the model as general as possible and to include communication latency associated with DR between the load aggregator companies (Lagcos) and the end-use customers' devices. This is an important parameter in the system dynamic performance of LFC-DR. We have assumed the communication delay between the balancing authority (BA) and the Lagcos to be the same as that between the BA and generation companies (Gencos). We have not considered these delays in our study since the focus of this paper is on the evaluation of the DR loop in the LFC model. The proposed LFC-DR also gives an opportunity to the system operator to choose the DR option or spinning/non-spinning reserve, or a combination of the two, based on the real-time market price. Furthermore, the LFC-DR model can be used to estimate the actual value of the required responsive load manipulation when the magnitude of the disturbance is unknown to the system operator.

Another motivation for this study is the importance of the dynamic performance of a power system with DR to provide AS. Several real cases of DR operation have revealed that extreme shedding of the responsive loads in emergency DR could lead to unexpected power oscillations, which complicate the sequential generation control [34], [35]. The LFC-DR model will help the operators to investigate the impact of DR on the dynamic performance of the system prior to its usage and during the automatic generation control (AGC) design process.

The idea of DR for AS used in this paper, has been fully explored in our previous work [21] and will not be repeated here. In such a model, the Lagcos will work with the customers and inform the utilities, e.g., independent system operators, of the amount of DR available. An example of such a model is the PJM electricity market [4].

The remainder of this paper is organized as follows: In Section II, the concept of LFC-DR model is developed for a single-area power system. The model is analytically evaluated in Section III. The controller design is presented in Section IV, and simulation results are given in Section V. Section VI includes a discussion of exceptional cases not explored in this paper and the future work. Finally, the paper is concluded in Section VII.

II. Problem Formulation for Single-Area Power System

The general low-order linearized power system model for the purpose of frequency control synthesis and analysis is given by the power balance equation in the frequency-domain [33], [36]:

$$\Delta P_T(s) - \Delta P_L(s) = 2H.s.\Delta f(s) + D.\Delta f(s) \quad (1)$$

where,

$\Delta P_T(s)$-$\Delta P_L(s)$ is the incremental power mismatch,
$\Delta f(s)$ is the frequency deviation,
$2H$ is the equivalent inertia constant,
D is the equivalent load-damping coefficient,
s is the Laplace transform operator.

Since DR for AS performs like spinning reserve in magnitude and power flow direction, i.e. once frequency deviation is negative (positive), it is required to turn OFF (ON) a portion of the responsive loads (i.e., DR), Eq. (1) can be simply modified as follows to include DR:

$$\Delta P_T(s) - \Delta P_L(s) + \Delta P_{DR}(s) = 2H.s.\Delta f(s) + D.\Delta f(s) \quad (2)$$

In some earlier works such as [25], [26], [31], the effect of DR has been included in the load-damping coefficient, D. We believe the effect of DR should be separated because D is an inherent parameter of the system and is not a controllable one, whereas DR is an intentional control signal. In addition, Eq. (2) will permit to have a separate control loop for DR, which is more realistic and gives a better structure for controller design. The block diagram for single-area power system with a simplified non-reheat steam turbine is shown in Fig. 1, where the feedback loop for DR is also shown. T_g and T_t are the equivalent speed-governor and turbine time constants, respectively, R is the equivalent droop value, and T_d is the equivalent DR delay. The parameters of the system can be the equivalent of all generation assets and load damping of the same area. This model is selected to convey the main idea of this paper. In our future work, this model will be extended to multi-area interconnected power systems with multiple Gencos and Lagcos.

Unlike the usual spinning reserve-provider power plants, there is no ramp up and down limitations on the DR resources. In other words, the power consumption status of controllable loads can be changed instantaneously by the command signal they receive. Therefore, the only obstacle for DR (disregarding the aggregation of small loads) is communication delay, known as latency, which could affect the system dynamic performance.

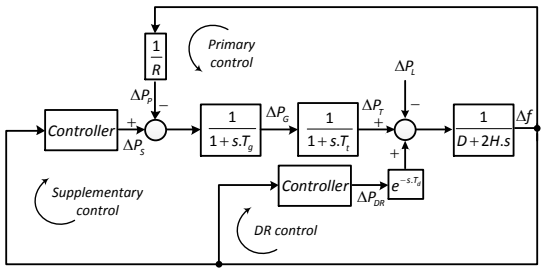

Fig. 1. Block-diagram representation of a single-area power system model

A. State-Space Dynamic Model for LFC-DR

State-space representation of the LFC model is a useful tool

for the application of modern/robust control theory [33]. It can also be used for creating a general framework of LFC in dynamic frequency analysis which can be conveniently modified and applied to power system of any size. We therefore derive the dynamic model of the power system, including DR in the state-space representation, to study the effect of DR on LFC performance and controller design. Although the proposed LFC-DR model of Fig. 1 is based on a simplified power system model with a non-reheat steam turbine, similar analysis and conclusions can be extended to other types of turbines, such as hydro or reheat-steam turbine.

The state-space realization of a single-area power system with DR (shown in Fig. 1) is given by:

$$\begin{aligned}\dot{\mathbf{x}}(t) &= \mathbf{A}.\mathbf{x}(t) + \mathbf{B}.\mathbf{u}(t) + \mathbf{\Gamma}.w(t)\\ y(t) &= \mathbf{C}.\mathbf{x}(t)\end{aligned} \tag{3}$$

where **A** is the system matrix, **B** is the control input matrix, **Γ** is the disturbance matrix, **x** is the state vector, **u**(*t*) is the input vector, *w*(*t*) is the disturbance variable, **C** is the observation matrix, and *y*(*t*) is the system output. In order to derive the linear state-space model of the system, it is required to have a linear model of the system under study. From Fig. 1, it can be seen that the system has only one nonlinear element which is the time delay in the DR control loop. Therefore, we need to linearize the time delay for derivation of the linear state-space model. *Padé* approximation, used for linearizing the DR time delay, is explained in the following sub-section.

B. Padé Approximation

Padé approximation has been widely used to linearize systems with time delays in control engineering with very strong convergent results [37]. It basically approximates time delays by a quotient of polynomials. Specifically, the *Padé* function for $e^{-s.T_d} \approx R_{pq}(-s.T_d)$ is defined as follows [38]:

$$R_{pq}\left(e^{-s.T_d}\right) = D_{pq}\left(e^{-s.T_d}\right)^{-1}.N_{pq}\left(e^{-s.T_d}\right) \tag{4}$$

where,

$$N_{pq}\left(e^{-s.T_d}\right) = \sum_{k=0}^{p} \frac{(p+q-k)!\,p!}{(p+q)!k!(p-k)!}.\left(-s.T_d\right)^k \tag{5}$$

$$D_{pq}\left(e^{-s.T_d}\right) = \sum_{k=0}^{q} \frac{(p+q-k)!\,q!}{(p+q)!k!(q-k)!}.\left(s.T_d\right)^k \tag{6}$$

N_{pq} and D_{pq} are polynomials of order *p* and *q*, respectively. It is usually common for the numerator and denominator of the approximation fractional functions to have the same order, and the order usually varies between 5 and 10 [37]. Fig. 2 shows the phase of the step response in frequency-domain of the *Padé* approximation with different orders in comparison to a pure time delay of 0.1 sec. Since the cut-off frequency of the low pass filters, i.e. speed-governor and turbine, in the model of the power system are usually less than 15 rad/sec, the 5th-order *Padé* approximation is acceptable and is used in this study. The magnitudes of all orders of *Padé* approximation in the frequency domain have also been compared to that of pure time delay. They are all at 0 dB and not shown here.

The signal flow graph for the state-space model of the power system shown in Fig. 1 with 5th-order *Padé* approximation is sketched in Fig. 3. The state variables are also shown in this figure for future reference. The gains of the feedback and feed-forward paths of the 5th-order *Padé* approximation are given in Table I. T_d is the DR communication latency.

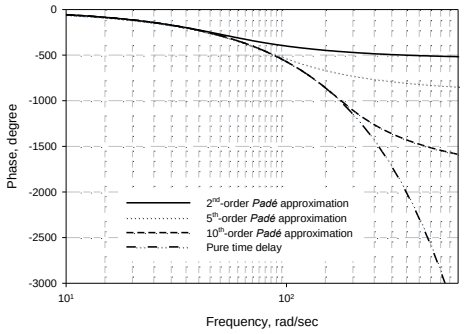

Fig. 2. Different order of *Padé* approximation for pure time delay, T_d=0.1 sec

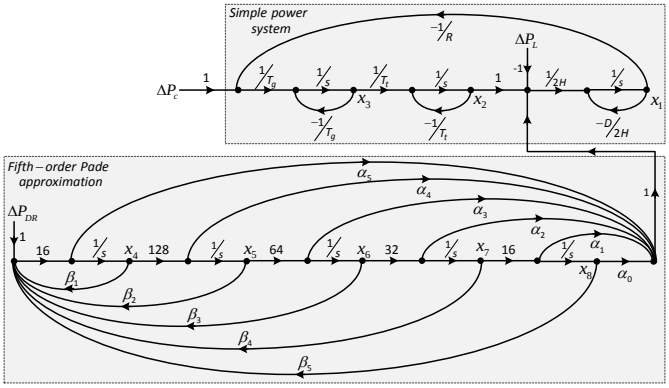

Fig. 3. Signal flow graph of the single-area power system model with 5th -order *Padé* approximation

TABLE I

Padé APPROXIMATIONS FEED-FORWARD AND FEEDBACK VALUES FOR SIGNAL FLOW GRAPH.

α_0	α_1	α_2	α_3	α_4	α_5
$945/2^{21}.T_d^5$	$-945/2^{22}.T_d^4$	$105/2^{17}.T_d^3$	$-105/2^{15}.T_d^2$	$15/2^9.T_d$	$-1/2^4$
	β_1	β_2	β_3	β_4	β_5
	$-15/2^3.T_d$	$-105/2^9.T_d^2$	$-105/2^{12}.T_d^3$	$-945/2^{18}.T_d^4$	$-945/2^{21}.T_d^5$

With the above approximation of time delay nonlinearity, the state-space representation of the system, Eq. (3), has the following matrices:

$$\mathbf{A} = \left[\begin{array}{ccc|ccccc} \frac{-D}{2H} & \frac{1}{2H} & 0 & \frac{30}{2H.T_d \times 2^3} & 0 & \frac{105}{2H.T_d^3 \times 2^{11}} & 0 & \frac{945}{2H.T_d^5 \times 2^{20}} \\ 0 & \frac{-1}{T_t} & \frac{1}{T_t} & 0 & 0 & 0 & 0 & 0 \\ \frac{-1}{R.T_g} & 0 & \frac{-1}{T_g} & 0 & 0 & 0 & 0 & 0 \\ \hline 0 & 0 & 0 & \frac{-30}{T_d} & \frac{-105}{T_d^2 \times 2^5} & \frac{-105}{T_d^3 \times 2^8} & \frac{-945}{T_d^4 \times 2^{14}} & \frac{-945}{T_d^5 \times 2^{17}} \\ 0 & 0 & 0 & 128 & 0 & 0 & 0 & 0 \\ 0 & 0 & 0 & 0 & 64 & 0 & 0 & 0 \\ 0 & 0 & 0 & 0 & 0 & 32 & 0 & 0 \\ 0 & 0 & 0 & 0 & 0 & 0 & 16 & 0 \end{array}\right] \tag{7}$$

$$\mathbf{B}^T = \left[\begin{array}{ccc|ccccc} 0 & 0 & \frac{1}{T_g} & 0 & 0 & 0 & 0 & 0 \\ \frac{-1}{2H} & 0 & 0 & 16 & 0 & 0 & 0 & 0 \end{array}\right] \tag{8}$$

$$\mathbf{\Gamma}^T = \left[\begin{array}{ccc|ccccc} \frac{-1}{2H} & 0 & 0 & 0 & 0 & 0 & 0 & 0 \end{array}\right] \tag{9}$$

$$\mathbf{C}=[1\ \ 0\ \ 0\ \vdots\ 0\ \ 0\ \ 0\ \ 0\ \ 0],\ D=[0] \tag{10}$$

where T is the transpose operation of matrices. For more complicated power systems, the upper left partition of matrix A, and the left partitions of other matrices can be modified to represent the new power system model. The other partitions of the matrices should be properly resized based on the order of the new power system model.

III. Analytical Evaluation of the Model

In this section, steady-state error evaluation, sensitivity analysis, and system stability of the LFC model with and without the DR control loop are presented.

A. Steady-State Error Evaluation

The primary control loop in Fig. 1, known as frequency droop control, is the fastest intentional control action in a power system but it is not enough to make the frequency deviation go to zero at steady-state. For this reason, the supplementary frequency control loop, as shown in Fig. 1, is required for further control. However, the DR control loop is also added to the problem in this study. Therefore, it is necessary to investigate the impact of the DR control loop on the steady-state error of the given power system in Fig. 1. Later in this sub-section, a synthesis of controller design, based on optimal sharing between DR and supplementary control loops, will be derived from the steady-state error evaluation.

The conventional LFC steady-state equations are well-documented, e.g. [33], [36]. Adding the DR control loop to the conventional LFC model, the system frequency deviation can be expressed as follows:

$$\Delta f(s)=\frac{1}{2H.s+D}\left[\Delta P_T(s)-\Delta P_L(s)+G(s).\Delta P_{DR}(s)\right] \tag{11}$$

where,

$$\Delta P_T(s)=H(s).\left[\Delta P_S(s)-\frac{1}{R}.\Delta f(s)\right],\ H(s)=\frac{1}{(1+s.T_g)(1+s.T_t)} \tag{12}$$

$$G(s)=\frac{-s^5+\frac{30}{T_d}.s^4-\frac{420}{T_d^2}.s^3+\frac{3360}{T_d^3}.s^2-\frac{15120}{T_d^4}.s+\frac{30240}{T_d^5}}{s^5+\frac{30}{T_d}.s^4+\frac{420}{T_d^2}.s^3+\frac{3360}{T_d^3}.s^2+\frac{15120}{T_d^4}.s+\frac{30240}{T_d^5}} \tag{13}$$

It can be seen that any type of power system model with equivalent turbine and governor can be represented by modifying $H(s)$. Substituting Eq. (12) into Eq. (11) yields:

$$\Delta f(s)=\frac{1}{2H.s+D}\left[H(s).\left[\Delta P_S-\frac{1}{R}.\Delta f(s)\right]-\Delta P_L(s)+G(s).\Delta P_{DR}(s)\right] \tag{14}$$

Solving Eq. (14) for $\Delta f(s)$ will result in the frequency deviation equation as follows:

$$\Delta f(s)=\frac{1}{\Psi(s)}.\left[H(s).\Delta P_S(s)+G(s).\Delta P_{DR}(s)\right]-\frac{1}{\Psi(s)}.\Delta P_L(s) \tag{15}$$

where,

$$\Psi(s)=2H.s+D+\frac{H(s)}{R} \tag{16}$$

In the LFC analysis, it is common to use a step load disturbance for $\Delta P_L(s)$ as:

$$\Delta P_L(s)=\frac{\Delta P_L}{s} \tag{17}$$

Based on the final value theorem, and substituting Eq. (17) into Eq. (15), the steady-state value of the system frequency deviation can be obtained as follows:

$$\Delta f_{SS}=\lim_{s\to 0} s.\Delta f(s)=\frac{\Delta P_{S,SS}+\Delta P_{DR,SS}-\Delta P_L}{\Psi(0)} \tag{18}$$

where,

$$\Delta P_{S,SS}=\lim_{s\to 0} s.H(s).\Delta P_S(s) \tag{19}$$

$$\Delta P_{DR,SS}=\lim_{s\to 0} s.G(s).\Delta P_{DR}(s) \tag{20}$$

$$\Psi(0)=D+\frac{H(0)}{R}=D+\frac{1}{R}\approx B \tag{21}$$

Therefore, $\Psi(0)$ is equivalent to the system frequency response characteristics, B, and the steady-state frequency deviation can be written as follows:

$$\Delta f_{SS}=\frac{\Delta P_{S,SS}+\Delta P_{DR,SS}-\Delta P_L}{D+1/R} \tag{22}$$

It can be seen from Eq. (22) that the frequency deviation will not be zero unless the supplementary and/or DR controls exist. Also, DR control loop gives an extra degree of freedom for system frequency regulation. In addition, the following conclusions can be drawn from Eq. (22):

- The steady-state error is not dependent on the delay and the order of its approximation,
- With DR available in the LFC, a higher reliability of frequency regulation can be achieved, since the DR control loop can complement the supplementary control loop. In cases when the supplementary control is not available, the performance of the frequency regulation can be guaranteed by the DR loop, if enough DR resources are available.
- In order to have zero frequency deviation at steady-state, the required control effort can be split between the supplementary and DR control loops. In other words, an ISO/RTO will have the opportunity to perform the regulation services in a cost effective way and analyze the frequency response of the system quickly. This goal can be achieved only in the proposed formulation (Eq. (22)) with an added control loop for DR (Fig. 1).

Further discussion to the last conclusion is: consider a situation where there is no DR available. The frequency error will be zero at steady-state if $\Delta P_{S,SS}=\Delta P_L$. It means that the supplementary control should provide enough spinning and/or non-spinning reserve at the time of disturbance. With DR available in the LFC, the required control effort, called Ω in this study, can be split between the two control loops based on their cost at real-time electricity market as follows:

$$\begin{cases}\Delta P_S(s)=\alpha.\Omega\\ \Delta P_{DR}(s)=(1-\alpha).\Omega\end{cases} \tag{23}$$

where $0<\alpha<1$ is the share of traditional regulation services in the required control effort. $\alpha=1$ means that the total required regulation will be provided by the traditional regulation services, i.e. spinning and non-spinning reserve, and $\alpha=0$ is for the time when all the required control would be provided by DR. The decision on the value of α should be made by the ISO/RTO, based on the price of DR and the traditional regulation services in a real-time market, explored by the authors in [21]. Then, it is possible for the ISO/RTO to effectively and quickly assess the different scenarios of LFC to

evaluate the system performance under various circumstances. Finally, the steady-state value of the two inputs should be:

$$\Delta P_{S,SS} = \alpha.\Delta P_L$$
$$\Delta P_{DR,SS} = (1-\alpha).\Delta P_L \quad (24)$$

B. Sensitivity Analysis for the Feedback System with and without DR

In this sub-section, an analytical method is utilized to study the impact of the DR control loop on the overall sensitivity of the closed-loop system w.r.t. the open-loop system. It is also desired to measure the sensitivity of the closed-loop system w.r.t. the coefficient α. The first sensitivity analysis is quite important since it shows the robustness of the closed-loop system performance when the system parameters are subjected to any change or variation. The second sensitivity analysis is also necessary since α is an important parameter in the performance of the LFC-DR model.

The power system model shown in Fig. 1 is modified for this part with a single integral controller (with gain *K*) for both the supplementary and DR control loops, and also for the rest of this paper, as shown in Fig. 4. This modification will also allow us to split the required control effort between the DR and supplementary control loops, as was discussed in sub-section III-A.

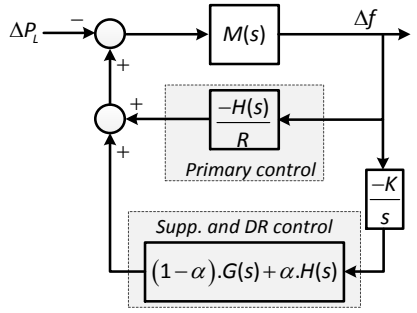

Fig. 4. Modified power system model with integral controller for DR and supplementary control loops

For the power system shown in Fig. 4, the closed-loop transfer function relating the system frequency deviation to a step change in the load can be derived as follows:

$$\left(\frac{\Delta f(s)}{\Delta P_L(s)}\right)_{DR} = \frac{-M(s)}{1+\frac{H(s).M(s)}{R}+\frac{K}{s}.\alpha.H(s).M(s)+\frac{K}{s}.(1-\alpha).G(s).M(s)}$$
$$\left(\frac{\Delta f(s)}{\Delta P_L(s)}\right)_{S} = \frac{-M(s)}{1+\frac{H(s).M(s)}{R}+\frac{K}{s}.H(s).M(s)} \quad (25)$$

where *K* is integral feedback gain of the system and $M(s)$ is

$$M(s) = \frac{1}{D+2H.s} \quad (26)$$

In Eq. (25), the first expression is the closed-loop transfer function when both DR and supplementary control loops are available, whereas the second equation shows the closed-loop transfer function for conventional LFC (with no DR). The open-loop transfer function, where only the primary control exists, can be derived as follows:

$$T_{OL}(s) = \left(\frac{\Delta f(s)}{\Delta P_L(s)}\right)_{OL} = \frac{-M(s)}{1+\frac{H(s).M(s)}{R}} \quad (27)$$

In order to derive the sensitivity function of the closed-loop system w.r.t. the open-loop system, Eq. (25) can be simplified and rearranged using Eq. (27):

$$T_{DR} = \left(\frac{\Delta f(s)}{\Delta P_L(s)}\right)_{DR} = \frac{1}{(T_{OL}(s))^{-1}-\frac{K}{s}.\alpha.H(s)-\frac{K}{s}.(1-\alpha).G(s)}$$
$$T_S = \left(\frac{\Delta f(s)}{\Delta P_L(s)}\right)_{S} = \frac{1}{(T_{OL}(s))^{-1}-\frac{K}{s}.H(s)} \quad (28)$$

Therefore, the unitless sensitivity function of the closed-loop system w.r.t. the open-loop system, for systems with and without DR, can be written as follows:

$$\mathbb{S}_{OL}^{DR} = \left(\frac{\partial T_{DR}/\partial T_{OL}}{T_{DR}/T_{OL}}\right) = \frac{(T_{OL}(s))^{-1}}{(T_{OL}(s))^{-1}-\frac{K}{s}.\alpha.H(s)-\frac{K}{s}.(1-\alpha).G(s)}$$
$$\mathbb{S}_{OL}^{S} = \left(\frac{\partial T_S/\partial T_{OL}}{T_S/T_{OL}}\right) = \frac{(T_{OL}(s))^{-1}}{(T_{OL}(s))^{-1}-\frac{K}{s}.H(s)} \quad (29)$$

It is noted from Eq. (29) that the closed-loop system is highly sensitive to the changes in the open-loop system, i.e. any change in the value of T_{OL} will have a large effect on $\mathbb{S}_{OL}^{DR}$ and $\mathbb{S}_{OL}^{S}$. From Eq. (29), the ratio of sensitivity functions can be expressed as:

$$\frac{\mathbb{S}_{OL}^{DR}}{\mathbb{S}_{OL}^{S}} = \frac{(T_{OL}(s))^{-1}-\frac{K}{s}.H(s)}{(T_{OL}(s))^{-1}-\frac{K}{s}.\alpha.H(s)-\frac{K}{s}.(1-\alpha).G(s)} \quad (30)$$

Eq. (30) can be rearranged as follows:

$$\frac{\mathbb{S}_{OL}^{DR}}{\mathbb{S}_{OL}^{S}} = \frac{\underbrace{(T_{OL}(s))^{-1}-\frac{K}{s}.H(s)}_{\Phi}-\underbrace{\frac{K}{s}.(1-\alpha)}_{\varphi}.G(s)+\frac{K}{s}.\alpha.H(s)}{\underbrace{(T_{OL}(s))^{-1}-\frac{K}{s}.\alpha.H(s)}_{\Phi}-\underbrace{\frac{K}{s}.(1-\alpha)}_{\varphi}.G(s)} = \frac{1-\frac{\varphi}{\Phi}.H(s)}{1-\frac{\varphi}{\Phi}.G(s)} \quad (31)$$

Therefore, it can be observed from Eq. (31) that the closed-loop LFC-DR is slightly less sensitive than the system without DR only if $H(s) > G(s)$, assuming Φ and φ have the same sign. In order to compare the sensitivity functions, a simulation study was carried out for an arbitrary integral feedback gain. The sensitivity values for both closed-loop systems are shown in Fig. 5. The values of the different parameters for this simulation study are given in Table II.

TABLE II
POWER SYSTEM PARAMETERS FOR THE SIMULATION STUDY [33].

T_g	T_t	R	$2H$	D	T_d	ΔP_L	K
0.08 sec	0.4 sec	3.0 Hz/p.u.	0.1667 pu. sec	0.015 p.u./Hz	0.1 sec	0.01 p.u.	0.2

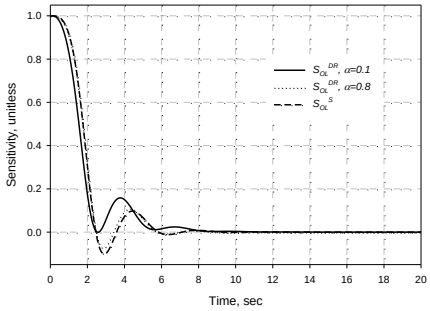

Fig. 5. The closed-loop system w.r.t. the open-loop system sensitivity values of a simulation study for LFC with and without DR

Two different values for α are used in Fig. 5 to show that a higher DR share (smaller α) will result in less sensitivity of the closed-loop system w.r.t the open-loop system. That is, the closed-loop system becomes less sensitive to the variation of uncertain parameters of the open-loop system. When α=0.8 (i.e., 80% of the required regulation would be provided by the supplementary control and 20% is from DR), the sensitivity values for both the closed-loop systems, with and without DR, are almost similar. This is a good indication that the 5th-order *Padé* approximation, used for linearizing the time delay in the DR loop, doesn't have any negative impact on the system performance. A similar study has been carried out to investigate the sensitivity of the closed-loop system w.r.t. the integral feedback gain, and similar results have been obtained.

Since α is an important parameter in the performance of the closed-loop system with DR, it is useful to evaluate the sensitivity of the closed-loop system w.r.t. this coefficient. The sensitivity function can be written as follows:

$$\mathbb{S}_{\alpha}^{DR}=\left(\frac{\partial T_{DR}/\partial\alpha}{T_{DR}/\alpha}\right)=\frac{\alpha.\frac{K}{s}.\left(H(s)-G(s)\right)}{\left(T_{OL}(s)\right)^{-1}-\frac{K}{s}.\alpha.H(s)-\frac{K}{s}.(1-\alpha).G(s)} \tag{32}$$

The previous simulation setup was utilized for two different values of α. Sensitivity results are shown in Fig. 6.

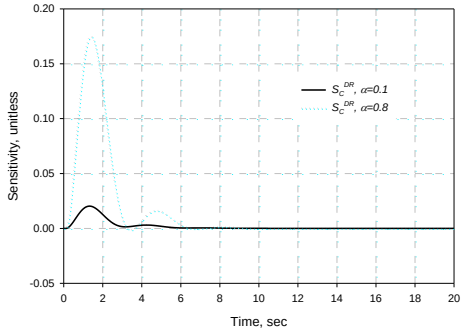

Fig. 6. The closed-loop system w.r.t. α sensitivity values for the LFC-DR model, α=0.1 and α=0.8

It can be seen from Fig. 6 that the closed-loop system is less sensitive to α when the DR control loop takes a higher share in the frequency regulation, i.e. smaller α values.

C. Stability Analysis of the Closed-Loop Systems

A prerequisite for satisfactory control of a feedback control system is its stability, and gain and phase margins are two criteria commonly used for stability evaluation [37]. The gain and phase margins can be obtained from the Bode diagrams of the open-loop transfer function of the closed-loop system since the zeros of the characteristic equation are poles of the closed-loop system [37]. Using the load disturbance, $\Delta P_L(s)$ as the system input, the open-loop transfer functions are:

$$\begin{aligned}&\underbrace{1+\frac{H(s).M(s)}{R}+\frac{K}{s}.\alpha.H(s).M(s)+\frac{K}{s}.(1-\alpha).G(s).M(s)=0}_{\vartheta^{DR}}\\&\underbrace{1+\frac{H(s).M(s)}{R}+\frac{K}{s}.H(s).M(s)=0}_{\vartheta^{S}}\end{aligned} \tag{33}$$

where ϑ^{DR} and ϑ^{S} are the open-loop transfer function for the closed-loop systems with and without DR, respectively. Here, the control characteristics of the closed-loop systems (Eq. (33)) can be obtained by taking the feedback gain as a variable parameter. From Eq. (33), it is possible to calculate the new open-loop transfer functions, $\hat{\vartheta}^{DR}$ and $\hat{\vartheta}^{S}$. These transfer functions have the same root-locus properties as of ϑ^{DR} and ϑ^{S} as follows:

$$\begin{aligned}&\underbrace{1+K.\frac{R.\left[\alpha.H(s).M(s)+(1-\alpha).G(s).M(s)\right]}{s.\left[R+H(s).M(s)\right]}=0}_{\hat{\vartheta}^{DR}}\\&\underbrace{1+K.\frac{R.H(s).M(s)}{s.\left[R+H(s).M(s)\right]}=0}_{\hat{\vartheta}^{S}}\end{aligned} \tag{34}$$

The Bode plots of the systems of Eq. (34) are shown in Fig. 7. The parameters of the case study are given in Table II. It can be seen from Fig. 7 that both systems (with and without DR) are relatively stable; however, larger gain and phase margins have been achieved when the DR control loop is added to the system. The phase and gain margins are given in Table III. It can be noticed from this table that a higher share of control effort for the DR control loop, i.e. smaller α, will provide a higher gain and phase margin, indicating a more stable system. In addition, the table shows that the 5th-order *Padé* approximation has no negative impacts on the stability of the system, as discussed in sub-section II-A.

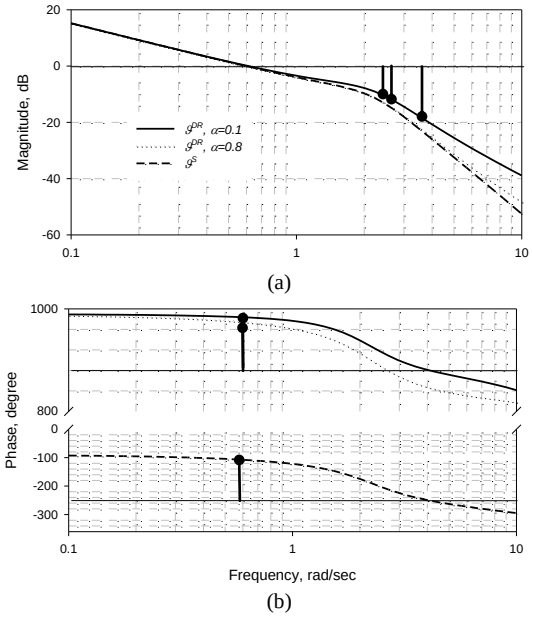

Fig. 7. Bode plot of the closed-loop systems for stability analysis, (a) magnitude, and (b) phase

TABLE III
PHASE AND GAIN MARGINS FOR THE OPEN-LOOP TRANSFER FUNCTION ASSOCIATED WITH EACH CLOSED-LOOP SYSTEMS.

	$\vartheta^{DR}, \alpha = 0.1$	$\vartheta^{DR}, \alpha = 0.8$	ϑ^{S}
Gain margin, *dB*	14.1	11.3	10.3
Phase margin, *degree*	83.5	74.8	72.2

IV. GENERAL APPROACH FOR CONTROLLER DESIGN FOR THE LFC-DR MODEL

Several different classical and modern control theories have been utilized for the LFC problem [32]. In this section, a general controller design approach for the LFC problem with the DR control loop is presented. Here, we use the widely used linear quadratic regulator (LQR) for controller design. We will examine other effective control design approaches, which will include parameter uncertainty and measurement noise, in our future work.

The simplified version of the LQR problem is to design the controller such that the performance index, Eq. (35), is minimized for the system given in Eq. (3) [39]:

$$\Im = \int_0^\infty \left[\mathbf{x}^T.\mathbf{Q}.\mathbf{x} + \rho.\mathbf{u}^T.\mathbf{R}.\mathbf{u} \right].dt \tag{35}$$

where ρ is a weighting factor chosen by the designer, considering the trade-off between system transient performance and control effort. $\mathbf{Q}$ is an *n*-by-*n* semidefinite symmetric state cost matrix (*n* is the number of system states), $\mathbf{R}$ is an *m*-by-*m* positive definite symmetric control cost matrix (*m* is the number of control inputs), and $\mathbf{x}^T = [x_1, \cdots, x_8]$ (where $x_1 = \Delta f, x_2 = \Delta P_g, x_3 = \Delta P$, and $x_4, \cdots, x_8$ are the states associated with the 5th-order *Padé* approximation).

Using Eq. (23), it can be shown that the control input to the supplementary controller ($u_1 = \Delta P_S$) and to the DR controller ($u_2 = \Delta P_{DR}$) are related as follows:

$$u_1 = \frac{\alpha}{1-\alpha}.u_2 \qquad or \qquad u_2 = \frac{1-\alpha}{\alpha}.u_1 \tag{36}$$

For the system with unified control inputs, all the state-space matrices will remain unchanged, except the control input matrix *B*, where Eq. (8) is modified to include $u_2 = F(u_1)$ as follows:

$$\hat{B}^T = \left[\frac{\alpha - 1}{2H.\alpha} \quad 0 \quad \frac{1}{T_g} \;\middle|\; \frac{16(1-\alpha)}{\alpha} \quad 0 \quad 0 \quad 0 \quad 0 \right] \tag{37}$$

It is also possible to use $u_1 = F(u_2)$ in Eq. (8). However, as will be shown in the simulation results in Section V, the system performances in the two cases are nearly identical.

It is also noted that all the system states are non-zero except Δf, where the goal is to keep Δf as close to zero as possible. As a result, the full-state feedback controller cannot guarantee zero steady-state error for frequency deviation. Therefore, an integral controller is necessary to ensure zero steady-state error in the system frequency. In the early works on the application of optimal control to the LFC problems, e.g. [40]-[43], it was common to fix this problem with redefining the states in terms of their steady-state values, which essentially needs a prior knowledge of the disturbance. However, in most real-world cases the disturbance to the power system is an unknown parameter. Therefore, in this study, an ad hoc solution to the integral control problem is utilized by augmenting the state vector [39]. The design will also be robust against any changes in the system parameters. Modifying the state-space model in Eq. (3) to include the integrator, the augmented state equations become:

$$\begin{bmatrix} \dot{\mathbf{x}} \\ \dot{x}_I \end{bmatrix} = \begin{bmatrix} \mathbf{A} & 0 \\ \mathbf{C} & 0 \end{bmatrix}.\begin{bmatrix} \mathbf{x} \\ x_I \end{bmatrix} + \begin{bmatrix} \hat{\mathbf{B}} \\ 0 \end{bmatrix}.\hat{u} + \begin{bmatrix} \mathbf{\Gamma} \\ 0 \end{bmatrix}.w$$
$$y = [\mathbf{C} \quad 0].\begin{bmatrix} \mathbf{x} \\ x_I \end{bmatrix} \tag{38}$$

where $\hat{u} = u_2$. The augmented state-space equation can be written as follows:

$$\dot{\tilde{\mathbf{x}}} = \tilde{\mathbf{A}}.\tilde{\mathbf{x}} + \tilde{\mathbf{B}}.\hat{u} + \tilde{\mathbf{\Gamma}}.w$$
$$\tilde{y} = \tilde{\mathbf{C}}.\tilde{\mathbf{x}} \tag{39}$$

where the states are defined as $\mathbf{x}^T = \left[\Delta f, \Delta P_g, \Delta P_t, x_4, \cdots, x_8, \int \Delta f.dt \right]$. The matrices for the modified system are:

$$\tilde{\mathbf{A}} = \left[\begin{array}{c|c} \mathbf{A} & \mathbf{0}_{8\times 1} \\ \hline [1 \quad \mathbf{0}_{1\times 7}] & 0 \end{array} \right], \tilde{\mathbf{B}}^T = \left[\hat{\mathbf{B}} \;\middle|\; 0 \right], \tilde{\mathbf{\Gamma}}^T = [\mathbf{\Gamma} \;|\; 0], \tilde{\mathbf{C}} = [\mathbf{C} \;|\; 0] \tag{40}$$

If the augmented system matrix is controllable, then the control law and the state feedback can be defined as:

$$\hat{u} = -[\mathbf{K} \quad K_I].\begin{bmatrix} \mathbf{x} \\ x_I \end{bmatrix} = -\tilde{\mathbf{K}}.\tilde{\mathbf{x}} \tag{41}$$

To employ the LQR method, it is required to define the state and control weighting matrices, $\mathbf{Q}$ and R (scalar quantity) respectively. Before defining the weighting matrices, a set of frequency response requirements should be defined:

- The steady-state frequency deviation following a step-change in the load must be zero, i.e. $[\Delta f]^2$ [40].
- The time error represented by the integral of the frequency deviation should not exceed ±3 seconds, i.e. $\left[\int \Delta f.dt \right]^2$ [40].

Eventually, the weighting matrices considering the above requirements will be as follows:

$$\mathbf{Q} = diag(1 \quad \mathbf{0}_{1\times 7} \quad 1), R = [1] \tag{42}$$

In the next section, simulation results for the LFC-DR model of a single-area power system are presented to verify the effectiveness of the proposed model.

V. SIMULATION RESULTS FOR SINGLE-AREA POWER SYSTEM

In order to show some important features of the proposed LFC-DR model, the results of several different simulation studies are reported in this section for a single-area power system. In order to make a fair comparison, similar LQR design procedure has been employed for controller design for both systems, with and without DR. The parameters used in the simulation studies are given in Table II. The LQR problem has been solved using MATLAB®/Control System Toolbox.

In the first simulation study, a 0.01 pu load disturbance was applied to the single-area power system with conventional LFC and the proposed LFC-DR model. The system frequency deviation is shown in Fig. 8.

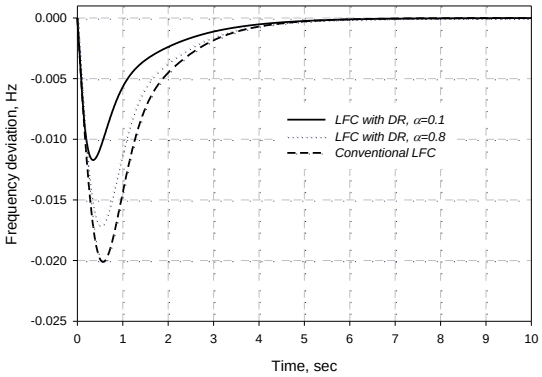

Fig. 8. Frequency deviation for conventional LFC and LFC-DR models

It can be seen that when α=0.1 (i.e., 10% of the required regulation is provided by the supplementary control and 90% from DR), the LFC-DR model has a superior performance over the conventional LFC during the transient period. Specifically, the overshoot in the system frequency deviation is decreased by about 42.5%. The results show improvement in the settling time as well. The same simulation was repeated for α=0.8. As expected, the lower DR control effort resulted in less improvement in the system dynamic performance. It can be observed that the dynamic performance of the system approaches that of conventional LFC for higher values of α.

The supplementary and DR control inputs are shown in Fig. 9, for the same simulation. As discussed in Section III.A, the steady-state values of the control inputs are based on the share between the DR and the supplementary control loops, i.e. the value of α, which is decided by the regional ISO/RTO based on the real-time electricity market. The steady-state value calculations are also shown in Fig. 9 which match with Eq. (24).

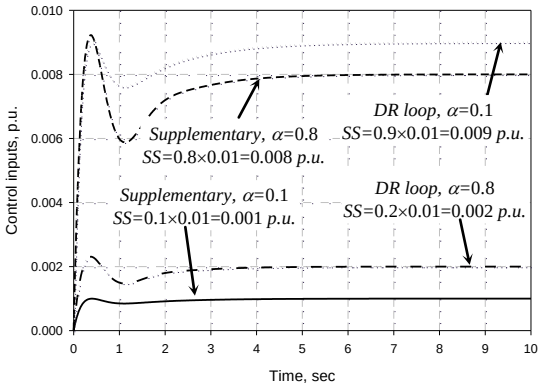

Fig. 9. Steady-state values of the control inputs for the LFC-DR model

A simulation study was carried out to show the impact of the order of *Padé* approximation on the performance of the system, the results of which are shown in Fig. 10. 2nd- and 5th-order *Padé* approximations are considered in the proposed LFC-DR model and compared with the conventional LFC, for α=0.1. It can be seen from Fig. 10 that the results from the 2nd- and 5th-order *Padé* approximation are almost identical. It is mainly because the simplified governor and turbine models are low pass filters which restrict the system response to lower frequency ranges, where *Padé* approximation is exactly the same as pure time delay, as discussed in Section II. Therefore, for simplicity, 2nd-order *Padé* approximation can be employed for more complicated power systems without negative impacts on the final results.

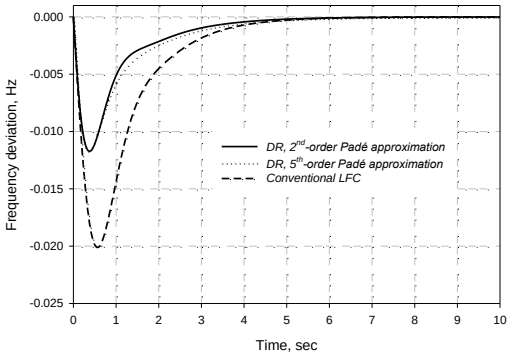

Fig. 10. Controller performance for different order of *Padé* approximation

As discussed in Section IV, the two control inputs are unified as a single input for the controller design as a function of α. The control input unification can be done in two ways: unifying $u_1(t)$ as a function of $u_2(t)$ or vice versa ($u_1 = \frac{\alpha}{1-\alpha}.u_2$ or $u_2 = \frac{1-\alpha}{\alpha}.u_1$). To show the impact of unification, a simulation study was carried out to compare the performance of the system for both unification cases, and the results are shown in Fig. 11. It can be observed that the difference between the two unifying approaches is negligible. In other words, the unifying control input can be chosen arbitrarily without any negative impact on the performance of the LFC-DR model.

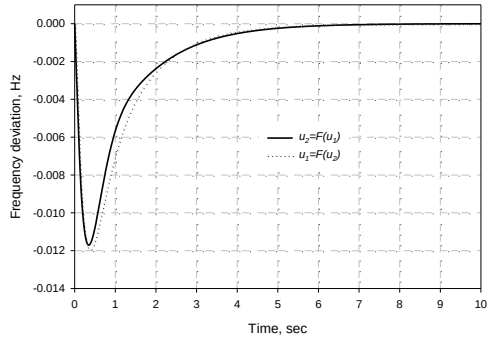

Fig. 11. The impact of different unified inputs on the performance of the LFC-DR model

One significant feature of the proposed LFC-DR model is the possibility for the ISO/RTO to evaluate the impact of communication delay of the DR control loop on the system performance for frequency stabilization. In order to show the impact of latency, a simulation study was performed for different values of communication latency for α=0.1. Simulation results are shown in Fig. 12. The lowest communication delay (lowest T_d) is for a small power system with fast two-way communication link, such as wireless communication, between the Lagcos and individual loads. It can be seen that the LFC-DR model gives a better performance compared to the conventional LFC when Td≤0.2 sec. When the time delay exceeds 0.2 sec, it deteriorates the performance of the LFC-DR, and the response is even worse than that of conventional LFC for Td=0.4 sec. This is not surprising since the single-area power system under study has a very fast dynamic response. In larger power systems with generation rate limiters and slow turbine-governor systems, a slower

dynamic behavior would be expected from the supplementary control. But, the LFC-DR will keep its superior performance even for higher communication latencies (discussed below).

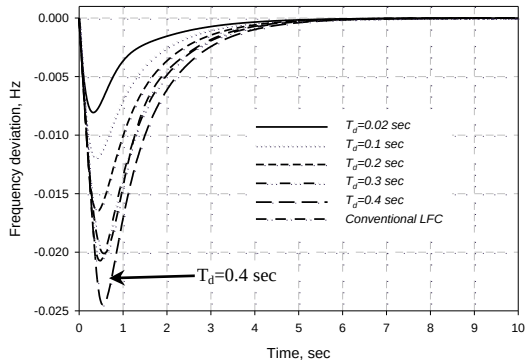

Fig. 12. The impact of latency on the performance of the LFC-DR model

To show the impact of the DR latencies on a larger power system with high inertia and slower response, another simulation study was conducted with the parameters given in Table IV. It can be seen from Fig. 13 that for a larger and consequently slower power system, the performance of the LFC-DR model is superior to that of conventional LFC even for larger communication latencies. It has been shown in [6] that even with the current Internet infrastructure, a latency of 500 msec can be achieved easily. Therefore, it can be concluded that the DR with the largest available latency (500 msec) still can be effective for large power systems.

TABLE IV
POWER SYSTEM PARAMETERS FOR THE SIMULATION STUDY [44].

T_g	T_t	R	$2H$	D	ΔP_L
0.3 sec	0.8 sec	2.4 Hz/p.u.	3.0 pu. sec	0.0083 p.u./Hz	0.01 p.u.

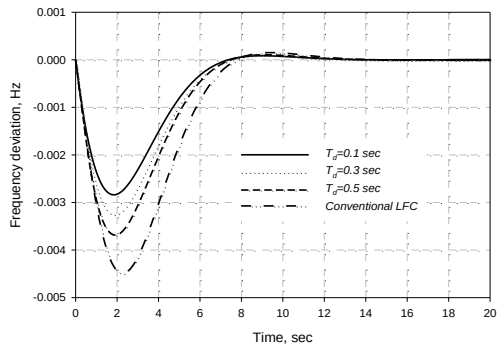

Fig. 13. The impact of DR latency on the performance of a slower single-area power system

VI. Discussion and Future Work

Our proposed LFC-DR model responds to all frequency deviations as is the case in the traditional LFC model [33], [36]. However, if it is desired to prevent the LFC-DR model to respond to small frequency deviations, and also keep the linearity of the model, a deadband could be added to the input, ΔP_L. ΔP_L could include the variation in any renewable generation that might be available in the power system as negative load. This is because of the fast dynamics of the common variable generation (wind, solar PV) compared to those of traditional power plants in the LFC model.

In this paper, we have explored the effectiveness of the LFC-DR model for frequency regulation at the transmission level in a single-area power system. However in general, large power systems are multi-area where different Gencos and Lagcos are available in each area. In our future work, we will report the application of LFC-DR in multi-area power systems.

VII. Conclusions

In this paper, a general framework is proposed to include DR into the LFC problem (LFC-DR). The proposed formulation can be expanded easily for any type of power system in size and characteristics. The framework adapts a real-time electricity market with existing load aggregators. It balances the power between generation and demand and stabilizes the system frequency by utilizing a percentage of available controllable loads and/or conventional supplementary control, based on the real-time market price. It also includes communication latencies in DR for controller design, using *Padé* approximation. It is shown through different analytical studies that the proposed LFC-DR framework will improve the stability margins in the conventional LFC model and is slightly less sensitive to the variation in the system parameters, such as changes in the open-loop transfer function. Similar results have also been obtained for the sensitivity of the closed-loop system w.r.t. the parameter α. Finally, the well-known LQR design is applied for full-state feedback controller design for a single-area power system. Simulation results show the effectiveness of the LFC-DR model in improving stabilization of the system frequency.

Acknowledgment

The fruitful discussion of the feedback control theory with Dr. Steven Shaw, Dr. Robert Gunderson of Montana State University, and Dr. Ali Gorji of University of Toronto is acknowledged.

References

[1] R. Doherty and M. O'Malley, "A new approach to quantify reserve demand in systems with significant installed wind capacity," *IEEE Trans. Power Syst.*, vol. 20, no. 2, May 2005, pp. 587–595.

[2] U.S. Department of Energy. (2011, September 28). Smart Grid [Online]. Available: http://energy.gov/oe/technology-development/smart-grid.

[3] C. Goldman, M. Reid, R. Levy, and A. Silverstein, "Coordination of energy efficiency and demand response a resource of the National Action Plan for Energy Efficiency," U.S Environmental Protection Agency and U.S. Department of Energy, Tech. Rep., 2010.

[4] R. Walawalkar, S. Blumsack, J. Apt, and S. Fernands, "An economic welfare analysis of demand response in the PJM electricity market," *Energ. Policy*, vol. 36, no. 10, Oct. 2008, pp. 3692–3702.

[5] M. Klobasa, "Analysis of demand response and wind integration in Germany's electricity market," *IET Renew. Power Gener.*, vol. 4, no. 1, Jan. 2010, pp. 55–63.

[6] A. Brooks, E. Lu, D. Reicher, C. Spirakis, and B. Weihl, "Demand dispatch: Using real-time control of demand to help balance generation and load," *IEEE Power Energy Mag.*, vol. 8, no. 3, May/June 2010, pp. 20–29.

[7] J. Medina, N. Muller, and I. Roytelman, "Demand response and distribution grid operations: Opportunities and challenges," *IEEE Trans. Smart Grid*, vol. 1, no. 2, Sept. 2010, pp. 193–198.

[8] H. Saele and O. S. Grande, "Demand response from household customers: Experiences from a pilot study in Norway," *IEEE Trans. Smart Grid*, vol. 2, no. 1, March 2011, pp. 102–109.
[9] N. Ruiz, I. Cobelo, and J. Oyarzaabal, "A direct load control model for virtual power plant management," *IEEE Trans. Power Syst*., vol. 24, no. 2, May 2009, pp. 959–966.
[10] A. J. Conejo, J. M. Morales, and L. Baringo, "Real-time demand response model," *IEEE Trans. Smart Grid*, vol. 1, no. 3, Dec. 2010, pp. 236–242.
[11] D. T. Nguyen, M. Negnevitsky, and M. de Groot, "Pool-based demand response exchange-concept and modeling," *IEEE Trans. Power Syst*., vol. 26, no. 3, Aug. 2011, pp. 1677–1685.
[12] P. Faria, Z. Vale, J. Soares, and J. Ferreira, "Demand response management in power systems using a particle swarm optimization approach," *IEEE Intell. Syst*., to be published.
[13] M. Parvania andM. Fotuhi-Firuzabad, "Integrating load reduction into wholesale energy market with application to wind power integration," *IEEE Syst. J*., vol. 6, no. 1, March 2012, pp. 35–45.
[14] K. Dietrich, J.M. Latorre, L.Olmos, A. Ramos, "Demand response in an isolated system with high wind integration," *IEEE Trans. Power Syst*., vol. 27, no. 1, Feb. 2012, pp. 20–29.
[15] M. Rastegar, M. Fotuhi-Firuzabad, and F. Aminifar, "Load commitment in a smart home," *J. Appl. Energy*, vol. 96, pp. 45–54, Aug. 2012.
[16] N. Navid-Azarbaijani and M. H. Banakar, "Realizing load reduction functions by aperiodic switching of load groups," *IEEE Trans. Power Syst*., vol. 11, no. 2, May. 1996, pp. 721–727.
[17] K. Y. Huang, H. C. Chin, and Y. C. Huang, "A model reference adaptive control strategy for interruptible load management," *IEEE Trans. Power Syst*., vol. 19, no. 1, Feb. 2004, pp. 683–689.
[18] D. Westermann and A. John, "Demand matching wind power generation with wide-area measurement and demand-side management," *IEEE Trans. Energy Convers*., vol. 22, no. 1, March 2007, pp. 145–149.
[19] S. A. Pourmousavi and M. H. Nehrir, "Demand response for smart microgrid: initial results," in *Proc*. 2nd *IEEE PES Innov. Smart Grid Technol*. (ISGT), California, 2011, pp. 1–6.
[20] S. A. Pourmousavi, M. H. Nehrir, and C. Sastry, "Providing ancillary services through demand response with minimum load manipulation," in *Proc. 43rd North Amer. Power Symp.* (NAPS), Massachusett, 2011, pp. 1–6.
[21] S. A. Pourmousavi and M. H. Nehrir, "Real-time central demand response for primary frequency regulation in microgrids," *IEEE Trans. Smart Grid*, Vol. 3. no. 4, Dec. 2012, pp. 1988-1996.
[22] D. Trudnowski, M. Donnelly, and E. Lightner, "Power-system frequency and stability control using decentralized intelligent loads," in *Proc*., *IEEE PES Conf. Exhib. Transm. Distrib*., Texas, 2005, pp. 1453–1459.
[23] J. A. Short, D. G. Infield, and L. L. Freris, "Stabilization of grid frequency through dynamic demand control," *IEEE Trans. Power Syst*., vol. 22, no. 3, Aug. 2007, pp. 1284–1293.
[24] A. Molina-García, F. Bouffard, and D. S. Kirschen, "Decentralized demand-side contribution to primary frequency control," *IEEE Trans. Power Syst*., vol. 26, no. 1, Feb. 2011, pp. 411–419.
[25] D. Jay, K.S. Swarup, "Dynamic demand response and control in smart grid environment," In *Proc*. *Annual IEEE India Conference* (INDICON), Hyderabad, 2011, pp. 1–4.
[26] D. Jay, K.S. Swarup, "Frequency restoration using dynamic demand control under smart grid environment," In *Proc. IEEE PES Innovative Smart Grid Technologies – India* (ISGT India), Kerala, 2011, pp.311–315.
[27] K. Samarakoon, J. Ekanayake, N. Jenkins, "Investigation of domestic load control to provide primary frequency response using smart meters," *IEEE Trans. Smart Grid*, vol. 3, no.1, March 2012, pp. 282–292.
[28] D. Angeli and P.-A. Kountouriotis, "A stochastic approach to dynamic demand refrigerator control," *IEEE Trans. Control Syst. Technol*., vol. 20, no. 3, May 2012, pp. 581–592.
[29] Z. Changhong, U. Topcu, S.H. Low, "Frequency-based load control in power systems," In *Proc*. *American Control Conference* (ACC), Canada, 2012, pp. 4423–4430.
[30] L.R. Chang-Chien, L.N. An, T.W. Lin, W.J. Lee, "Incorporating demand response with spinning reserve to realize an adaptive frequency restoration plan for system contingencies," *IEEE Trans. Smart Grid*, vol. 3, no. 3, Sept. 2012, pp. 1145–1153.
[31] H. Huang, F. Li, "Sensitivity analysis of load-damping characteristic in power system frequency regulation," *IEEE Trans. Power Syst*., vol. 28, no. 2, May 2013, pp. 1324–1335.
[32] Ibraheem, P. Kumar, D.P. Kothari, "Recent philosophies of automatic generation control strategies in power systems," *IEEE Trans. Power Syst*., vol. 20, no. 1, Feb. 2005, pp. 346–357.
[33] H. Bevrani, *Robust Power System Frequency Control*, New York: Springer, 2009, ch. 1–3.
[34] C.-C. Wu, W.-J. Lee, C.-L. Cheng, and H.-W. Lan, "Role and value of pumped storage units in an ancillary services market for isolated power system-simulation in the Taiwan power system," *IEEE Trans. Ind. Appl*., vol. 44, no. 6, Nov/Dec 2008, pp. 1924–1929.
[35] J.Mickey, "Using load resources to meet ancillary service requirements in the ERCOT market: A case study," in *Proc. IEEE PES Gen. Meet*., Minnesota, 2010, pp. 1-2.
[36] P. Kundur, *Power system Stability and Control*, New York: McGraw-Hill, 1994, ch. 11.
[37] R.C. Dorf, R.H. Bishop, *Modern Control Systems*: 7th ed., New York: Addison-Wesley Publishing Company, 1995, p. 807.
[38] G.H. Golub, C.F. Van Loan, *Matrix Computations*: 3rd ed., Baltimore: The Johns Hopkins University Press, 1996, pp. 572-574.
[39] G.F. Franklin, J.D. Powell, A. Emami-Naeini, *Feedback Control of Dynamic Systems*, 3rd ed., New York: Addison-Wesley Publishing Company, 1994, p. 778.
[40] C.E. Fosha, O.I. Elgerd, "The megawatt-frequency control problem: A new approach via optimal control theory," *IEEE Trans. Power Ap. Syst.*, vol. PAS-98, no. 4, April 1970, pp. 563–577.
[41] E.C. Tacker, C.C. Lee, T.W Reddoch, T.O. Tan, P.M. Julich, "Optimal control of interconnected electric energy systems: a new formulation," *IEEE Proc. letters*, vol. 60, no. 10, Oct. 1972, pp.1239–1241.
[42] G. Shirai, "Load frequency control using Lyapunov's second method: Bang-bang control of speed changer position," *IEEE Proc. letters*, vol. 67, no. 10, Oct. 1979, pp.1458–1459.
[43] S.C. Tripathy, T.S. Bhatti, C.S. Jha, O.P. Malik, G.S. Hope, "Sampled data automatic generation control analysis with reheat steam turbines and governor dead-band effects," *IEEE Trans. Power Ap. Syst.*, vol. PAS-103, no. 5, May 1984, pp. 1045–1051.
[44] T. Hiyama, "Design of decentralized load-frequency regulators for interconnected power systems," In *Proc*. *IEE Generation, Transmission, and Distribution conf.*, vol. 129, no. 1, 1982, pp. 17–23.

BIOGRAPHIES

S. Ali Pourmousavi (S'07) received the B.S. degree with honors from University of Mazandaran, Iran in 2005 and M.S. degree with honors from Amirkabir University of Technology (Tehran Polytechnic), Iran in 2008, all in electrical engineering. He is a Ph.D. student in the Electrical and Computer Engineering (ECE) Department at Montana State University, Bozeman, MT. His research interests include energy management of hybrid power generation systems, load control and demand response, and wind speed and power forecasting.

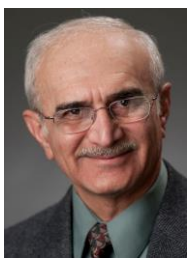

M. Hashem Nehrir (S'68–M'71–SM'89–F'10) received the B.S., M.S., and Ph.D. degrees from Oregon State University, Corvallis, in 1969, 1971, and 1978, respectively, all in electrical engineering. He was with the Electrical Engineering Department, Shiraz University, Iran from 1971 to 1986. Since 1987, he has been on the faculty of the Electrical and Computer Engineering Department, Montana State University, Bozeman, MT, where he is a Professor. His research interests include modeling and control of power systems, alternative energy power generation systems, and application of intelligent controls to power systems. He is the author of three textbooks and an author or coauthor of numerous technical papers.